Direct Observation of Alkali Metal Ion Recognition Processes at the Heptane/Water Interface by Second Harmonic Generation Spectroscopy

Kimihisa Nochi, Akira Yamaguchi, Takashi Hayashita, Tatsuya Uchida,† and Norio Teramae*

Department of Chemistry, Graduate School of Science, Tohoku University, Aoba-ku, Sendai 980-8578, Japan

Received: May 16, 2002; In Final Form: July 17, 2002

Alkali metal ion recognition with [2-hydroxy-5-(4-nitrophenylazo)phenyl]-methyl-15-crown-5 (azoprobe **1**) at the heptane/water interface was investigated by in situ second harmonic generation (SHG) spectroscopy. Upon addition of alkali metal ions, the second harmonic (SH) intensity of azoprobe **1** at the heptane/water interface was found to increase selectively. The observed selectivity of $K^+ > Na^+ > Li^+ > TMA^+$ was essentially the same order as that of the extractability for alkali metal ions in the 1,2-dichloroethane/water extraction. Although the Li^+ extractability by azoprobe **1** was very low in the 1,2-dichloroethane/water system, the observed increase of SH intensity suggested that the Li^+ complex could distribute to some extent at the heptane/water interface. The red shift of the SHG spectra for azoprobe **1** revealed that the heptane/water interface had an intermediate polarity between those of the two solvents. The light polarization analysis of the SH intensity exhibited a clear orientation change of azoprobe **1** at the heptane/water interface on forming the alkali metal complexes. It was experimentally clarified that the Na^+ and K^+ complexes were flatter while the Li^+ complex exhibited a lift-up orientation as compared with the free anionic azoprobe **1** at the heptane/water interface.

Introduction

Recent spectroscopic investigations on liquid/liquid and liquid/air interfaces have revealed that characteristics of the interface such as polarity,[1−4] hydrogen-bonding structure,[5,6] interfacial roughness,[7] and molecular association[8] are apparently different from those in bulk solutions. By using these unique physicochemical characteristics of interfaces, novel molecular recognition systems have been developed.[9−15] To understand molecular recognition at liquid interfaces on a molecular level, the adsorption and orientation changes of host molecules induced by the recognition process must be clarified. Such information would provide a novel design concept for molecular recognition at liquid interfaces in relation to mimicking biological membrane processes. However, in many cases, molecular recognition at the liquid interfaces has been evaluated by indirect analysis such as surface pressure, interfacial tension, and electrochemical techniques.[9,13,16−19] Although structural information on molecular recognition systems at liquid/air interfaces can be obtained from FTIR-RAS and XPS,[9] there have been only a few spectroscopic studies[20,21] for molecular recognition at liquid/liquid interfaces due to experimental difficulty in separation of the optical response of adsorbates from that of bulk molecules.

Second harmonic generation (SHG) spectroscopy has recently received much attention as a powerful tool for evaluating interfacial phenomena, due to its inherent sensitivity toward molecules at the interfaces.[22−26] Since the SH signal is significantly enhanced when the incident laser wavelength, and/or its SH wavelength, is in resonance with an electronic absorption of the molecules, electronic structures of interfacial species can be specifically analyzed.[3,27−29] At liquid/liquid interfaces, therefore, SHG spectroscopy can provide information on a molecular level for such items as orientation,[30] chemical equilibria,[28] molecular ordering,[31] and molecular association.[8] In addition, interfacial polarity can be elucidated for a variety of liquid interfaces from the SHG spectra utilizing solvatochromic probes.[2,3]

In this study, the dynamic properties of distribution and orientation changes for [2-hydroxy-5-(4-nitrophenylazo)phenyl]-methyl-15-crown-5 (azoprobe **1**, Figure 1A) upon complexation with alkali metal ions at the heptane/water interface have been examined by SHG spectroscopy. Azoprobe **1** has already been reported as a useful extraction spectrophotometric reagent for selective alkali metal ion recognition.[32] Then, the proton-dissociated form of azoprobe **1** exhibits a high water solubility and hardly any extracts into the heptane phase. Since the concentration of azoprobe **1** is negligibly small, influence from the absorption of fundamental and SH light passing through the heptane phase can be disregarded, and hence the alkali metal ion recognition by azoprobe **1** at the heptane/water interface can be clearly assessed by SHG spectroscopy (Figure 1B). The alkali metal ion selective distribution and orientation changes of azoprobe **1** at the heptane/water interface are experimentally clarified in the present SHG analysis.

Experimental Section

Apparatus. The SHG spectroscopy setup has been described previously.[8] The visible laser radiation from an optical parametric generator (Ekspla 410VIR) pumped by a picosecond Nd:YAG laser (Ekspla PL2143B) was incident on the heptane/water interface, and its polarization was controlled by a polarizer and Fresnel's rhomb. The SHG output from the interface was separated from the fundamental beam and extraneous emission from the interface using an optical filter, and then its polarization was selected by the polarizer. The intensity of the SH light was

* Author to whom correspondence should be addressed. E-mail: tera@anal.chem.tohoku.ac.jp.

† Present Address: School of Life Science, Tokyo University of Pharmacy and Life Science, Hachioji 192-0392, Japan.

10.1021/jp026122q CCC: $22.00
Published on Web 08/30/2002

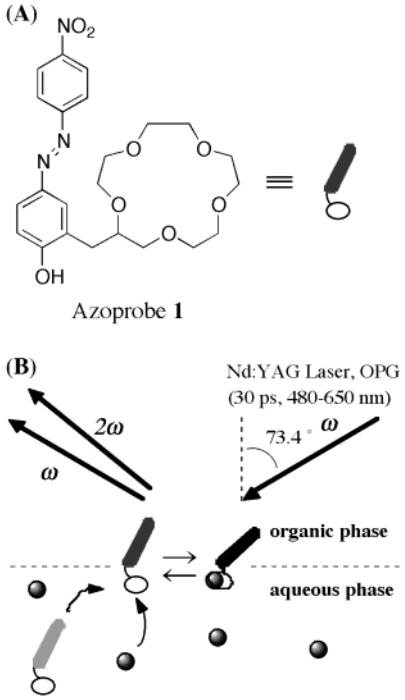

Figure 1. (A) Structure of [2-hydroxy-5-(4-nitrophenylazo)phenyl]-methyl-15-crown-5. (B) Schematic representation of SHG spectroscopy at heptane/water interface.

detected by a photomultiplier tube (Hamamatsu R928) attached to a monochromator (Nikon P-250). Data were finally processed with a digital oscilloscope (Tektronix TDS524A) and all data were corrected for the wavelength dependence of the laser source power. The incident angle was fixed to 74.3° to obtain the total internal reflection geometry. Typical laser power was 0.6 mJ/cm^2. All spectral measurements were carried out at room temperature.

Reagents. Synthesis of azoprobe **1** has been reported elsewhere.[32] Tetramethylammonium chloride (TMACl) (>98.0%), LiCl (>98.0%), NaCl (>99.5%), KCl (>99.5%), tetramethylammonium hydroxide (TMAOH) (15 ± 1 wt % aqueous solution), and heptane(>99.0%) were purchased from Wako Pure Chemical Industries, Ltd., and used without further purification. Water was distilled twice and then purified with a Millipore Milli-Q system.

Results and Discussion

UV−Visible Absorption Spectra of Azoprobe 1 in Bulk Water. The effect of alkali metal species upon UV−Vis spectra of azoprobe **1** in water is examined first. Absorption spectra of azoprobe **1** (1.0×10^{-6}) in water containing 0.10 M TMACl or alkali metal chlorides (LiCl, NaCl, KCl) are shown in Figure 2A(a)−(d). The pH of all sample solutions is adjusted to 11.8 by 0.01 M TMAOH. Since a crown ether binding site has no interaction with TMA^+ ion, TMA^+ salt is selected as a blank reference. The observed absorption maxima are 495.5 nm for TMACl, 494.0 nm for LiCl, 493.5 nm for NaCl, and 494.0 nm for KCl, and no meaningful salt effect is recognized in the UV−Vis spectra of azoprobe **1** in water. Since the pK_a of azoprobe **1** is reported to be 7.97 in water,[32] the main species of azoprobe **1** in 0.01 M TMAOH (pH = 11.8) must be the proton-dissociated form. Thus only two species, free anionic species (L^-) and alkali metal complex species (ML), are considered to exist in the sample solutions. The absorption bands observed for azoprobe **1** are ascribed to the $\pi-\pi^*$ transitions of L^- and

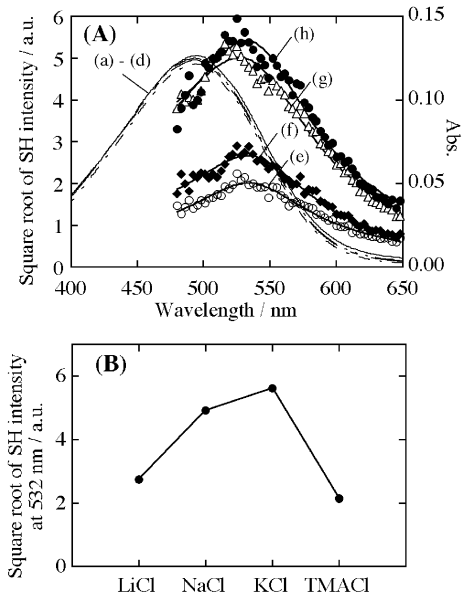

Figure 2. (A) UV−Vis spectra of 1.0×10^{-6} M azoprobe **1** in bulk water (pH 11.8) containing 0.10 M (a) TMACl, (b) LiCl, (c) NaCl, and (d) KCl. SHG spectra of 1.0×10^{-6} M azoprobe **1** at the heptane/water interface containing (e) TMACl, (f) LiCl, (g) NaCl, and (h) KCl. (B) Square root of SH intensity for each guest ion.

ML. When the 1:1 stability constant of azoprobe **1** in water is nearly equal to that of 15-crown-5 (5.5 M^{-1} for K^+, 5.0 M^{-1} for Na^+, and ≅0 for Li^+),[33] the concentration ratio of L^- to ML in 0.10 M alkali metal sample solution is estimated to be 1:1 for K^+ and Na^+, while only the L^- species exists for Li^+. Therefore the results observed in Figure 2 indicate that the electronic state of L^- is nearly the same as that of the ML species, so that the molecular hyperpolarizability of L^- is almost the same as that of the ML complexes.

SHG Spectra of Azoprobe 1 at the Heptane/Water Interface. The SHG analyses are carried out at the heptane/water interface, in which the aqueous sample solution contains 1.0×10^{-6} M azoprobe **1** and 0.10 M TMACl or alkali metal chlorides, and the solution pH's are adjusted to 11.8 by 0.01 M TMAOH. The SHG spectra of azoprobe **1** (L^- and ML species) at the heptane/water interface can be obtained from the wavelength dependence of the SH intensity ($I_{2\omega}$), expressed by the following equations: [2,3]

$$I_{2\omega} \propto |\chi_s^{(2)}|^2 I_\omega{}^2 \tag{1}$$

$$\chi_s^{(2)} = \frac{a}{\frac{1}{\lambda_{max}} - \frac{1}{\lambda} + i\Gamma} + b \tag{2}$$

where I_ω is the fundamental intensity and $\chi_s^{(2)}$ represents the second-order susceptibility. The terms, a, b, Γ, and λ_{max} are the resonance amplitude of the resonant and nonresonant parts of $\chi_s^{(2)}$, the line width, and the wavelength of the electronic transition, respectively. The fundamental wavelength of incident visible laser is λ. Since the SH signal of azoprobe **1** adsorbed at the heptane/water interface is large, the contribution from nearby solvent molecules can be neglected.[23] In addition, since molar absorptivity of the probe molecule at the fundamental wavelength is much larger than that at the SH wavelength, only the resonant part at the fundamental wavelength is taken into consideration.

The SHG spectra of azoprobe **1** at the heptane/water interface recorded under the condition of *s*-polarized fundamental input

and *p*-polarized SHG output are shown in Figure 2A(e)−(h). For the SH intensity range shown in Figure 2A, no significant SH signal was observed in the absence of azoprobe **1** in water. Thus, the observed SHG spectra in Figure 2A are strong evidence that azoprobe **1** molecules are adsorbed at the heptane/water interface as SHG active species. The SHG spectra of azoprobe **1** at the heptane/water interface exhibit a clear red shift in comparison with the UV−Vis absorption peaks in bulk water. The values of λ_{max} determined from fitting analysis of the SHG spectra by eq 2 are 540 ± 2 nm for TMACl, 542 ± 2 nm for LiCl, 540 ± 3 nm for NaCl, and 541 ± 3 nm for KCl, indicating the red shift of ca. 45 nm from the UV−Vis absorption peaks in bulk water.

The distribution measurement shows that the percent extraction of azoprobe **1** (L^- and ML) from aqueous phase (pH = 11.8) containing 0.10 M TMACl or alkali metal chlorides into heptane is less than 1%. Thus, absorption of the fundamental light and the SHG signals by azoprobe **1** in the heptane phase is negligible. As reported in previous paperes,[2,34] the interference of resonant and non resonant parts in the second-order susceptibility causes a difference in the observed wavelength peaks between UV−Vis and SHG spectra. However, in the present calculation, eq 2 already includes the interference effect, so that the calculated red shift must be due to other factors. Since the absorption spectrum of a molecule whose structure is similar to azoprobe **1** is known to exhibit the red shift in nonpolar solvents such as 50% aqueous dioxane,[35] the red shift observed for azoprobe **1** at the heptane/water interface is ascribed to a negative solvatochromism induced by different polarities between the heptane/water interface and bulk water. This indicates that the polarity at the heptane/water interface is lower than that in the bulk water, which is consistent with the results reported by Wang et al.[3]

It is also possible that the aggregation of azoprobe **1** at the heptane/water interface causes the spectral shift of azoprobe **1** due to the exciton coupling.[36] However, no SHG spectral shifts occur upon addition of alkali metal salts for azoprobe **1** at the heptane/water interface which excludes the self-aggregation of azoprobes adsorbed at the interface.

As shown in Figure 2A(e)−(h), the SH intensity of azoprobe **1** is found to significantly increase upon addition of alkali metal salts; the intensity dependence at 532 nm on ionic species is shown in Figure 2B. To evaluate this increase in the SH intensity, two species (L^- and ML) at the heptane/water interface must be considered as the SHG active species. The square root of SH intensity ($\sqrt{I_{2\omega}}$) is expressed by eq 3:[23,28,37]

$$\sqrt{I_{2\omega}} \propto \chi_{s,IJK}^{(2)} = N_{s,L^-}\langle\beta_{L^-}\rangle + N_{s,ML}e^{i\Delta\phi}\langle\beta_{ML}\rangle_{ijk} \quad (3)$$

where $\chi_{s,IJK}^{(2)}$ is the element of the second-order susceptibility, and N_{s,L^-} and $N_{s,ML}$ denote the interfacial concentrations of L^- and ML. β_{L^-} and β_{ML} are the molecular hyperpolarizabilities of L^- and ML, $\Delta\phi$ is the difference in phase angles between the hyperpolarizability tensor elements of L^- and ML. The $\langle\beta\rangle_{ijk}$ is a simple expression of $\langle T(\theta,\phi,\varphi)\rangle\beta_{ijk}$, where $\langle T(\theta,\phi,\varphi)\rangle$ is the transformation tensor between the molecular and the laboratory frames. The molecular frame is referenced with Euler's angles θ, ϕ, and φ (Figure 3).

Equation 3 clearly indicates that the factors affecting the SH intensity are (i) the difference in the molecular hyperpolarizability of ML species compared with L^-; (ii) the influence of $\Delta\phi$; (iii) the orientational change by ML complex formation; and (iv) the concentration change of L^- and ML species at the heptane/water interface. Since absorption spectral features of azoprobe **1** do not depend on alkali metal ions and TMA^+ (Figure 2A), the molecular hyperpolarizability of L^- is almost the same as that of ML complex, and hence the effect of $\Delta\phi$ upon the SH intensity is negligible. In addition, since the influence of the orientational change upon the SH intensity is estimated to be small, the increase in the SH intensity observed in Figure 2A is mainly attributable to the increase in ML concentration at the heptane/water interface.

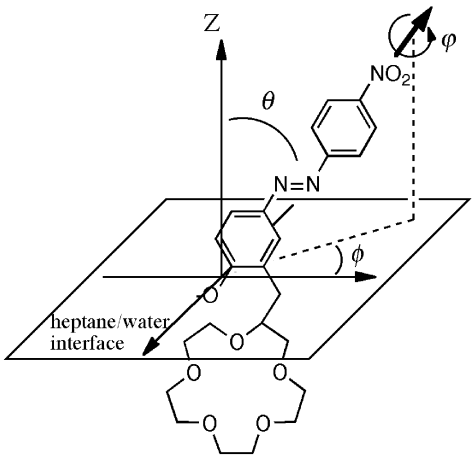

Figure 3. Definition of the angles θ, ϕ, and φ. The surface normal is defined as the *Z*-axis.

SCHEME 1: Equilibria between the Aqueous Phase and the Heptane/Water Interface[a]

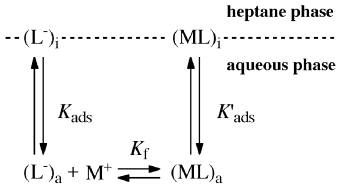

[a] K_{ads} and K'_{ads} are adsorption coefficients of L− and ML, respectively. K_f is a binding constant of L−.

TABLE 1: Extraction Constants K_{ex} with Selectivity Ratios (1,2-dichloroethane/water, 25 °C)

−log K_{ex} (ratio)		
Li^+	Na^+	K^+
—[a]	10.08 (0.59)	9.84 (1)

[a] The metal ion was not extracted.

Scheme 1 shows the equilibria of L^- and ML species between the aqueous phase and the heptane/water interface. It is evident that the larger stability constant (K_f) and the larger adsorption coefficient of ML species (K'_{ads}) cause a significant increase in ML concentration at the interface, resulting in the enhancement of the SH intensity. This behavior is very similar to that of the solvent extraction system.[38] The extraction behavior of azoprobe **1** for alkali metal ions from the aqueous phase into 1,2-dichloroethane has been examined and the extractabilities are summarized in Table 1.[32] The comparison of SH intensity change upon addition of alkali metal ions with the extractability of azoprobe **1** reveals that the increase of SH intensity is strongly dependent on the extraction selectivity of azoprobe **1** for alkali metal ions. This is clear evidence that the ML complexes are selectively adsorbed at the heptane/water interface. It should be noted that the SH intensity for LiCl increases slightly in comparison with the TMACl system, though the extractability of azoprobe **1** for LiCl is very low in the 1,2-dichloroethane/water extraction. This suggests that the Li^+ complex distributes

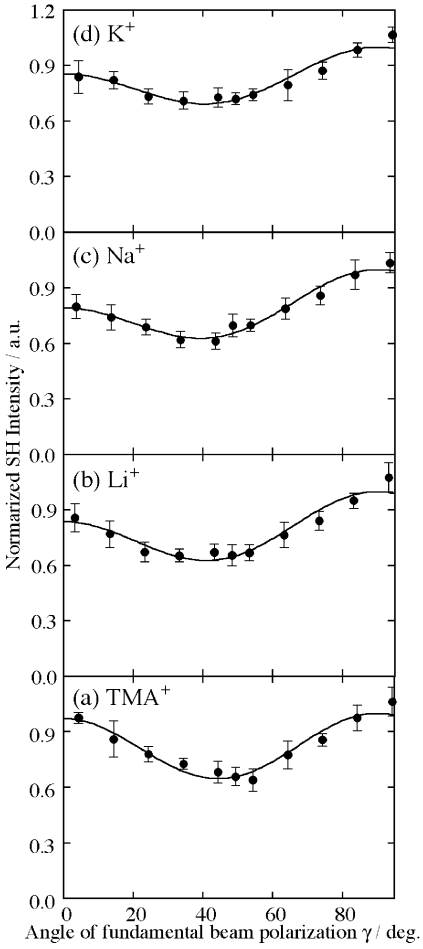

Figure 4. *p*-polarized SHG from azoprobe **1** at the heptane/water interface for each guest ion: (a) TMA^+, (b) Li^+, (c) Na^+, (d) K^+. The solid lines are theoretically fitted curves obtained using eq 5.

to some extent at the heptane/water interface. Since the heptane/water interface has an intermediate polarity between those of the two solvents,[1−4] even the hydrated Li^+ complex may be stabilized by specific solvation at the liquid/liquid interface.

Orientation of Azoprobe 1 at the Heptane/Water Interface. Molecular orientations of L^- and ML species at the heptane/water interface can be estimated by a light polarization analysis of the SH intensity. On the assumption that the two species of azoprobe **1** (L^- and ML) adsorbed at the heptane/water interface are randomly distributed in terms of rotation around the surface normal, the second-order susceptibility has only three elements of χ_{xxz}, χ_{zxx}, and χ_{zzz}.[30] The intensity of the *s*-polarized and *p*-polarized SH signals ($I_s(2\omega)$ and $I_p(2\omega)$) are expressed by the following relations:[30]

$$I_s(2\omega) \propto |a_1\chi_{xxz}\sin 2\gamma|^2 I(\omega)^2 \quad (4)$$

$$I_p(2\omega) \propto |(a_2\chi_{xxz} + a_3\chi_{zxx} + a_4\chi_{zzz})\cos^2\gamma + a_5\chi_{zxx}\sin^2\gamma|^2 I(\omega)^2 \quad (5)$$

where γ is the polarization angle of the incident light ($\gamma = 0°$ for *p*-polarized light, and $\gamma = 90°$ for *s*-polarized light). The a_n ($n = 1-5$) are the Fresnel coefficients depending on both the incident angle and the relative optical dielectric constants.

Figure 4 represents the *p*-polarized SH intensity as a function of the polarization angle of the incident light at 532 nm, which is nearly the peak position of the SHG spectra. In this figure, only *p*-polarized SHG curves are drawn because the overall *s*-polarized SH intensity only changes monotonically in all sample solutions. In Figure 4, each polarization curve is normalized to the maximum SH intensity obtained from theoretical fitting by eq 5. As compared with the result for TMA^+, the SH intensity in the vicinity of $\gamma = 0°$ decreases in the presence of alkali metal ions. In addition, the decrease in the SH intensity at around $\gamma = 45°$ is small for K^+. These differences observed for the *p*-polarized SHG curves indicate that the orientation of azoprobe **1** at the heptane/water interface changes by selective complex formation with alkali metal ions.

Since hyperpolarizability of azobenzene dyes is known to be dominated by a single element β_{zzz}, which is an element of the hyperpolarizability along the $\pi-\pi^*$ moment derection,[28,30] β_{zzz} for azoprobe **1** is taken into account as an effective element in the analysis of molecular orientation. In this case, the orientation parameter *D* can be determined from the second-order susceptibility elements obtained from the fitting of polarization curves with eqs 4 and 5.[30] On the assumption that a sharp distribution of orientation takes place at the interface, the orientation angle θ for L^- can be estimated from the result for the TMA^+ system according to eq 6.[30]

$$D = \frac{\langle\cos^3\theta\rangle}{\langle\cos\theta\rangle} = \frac{\chi_{zzz}}{\chi_{zzz} + 2\chi_{xxz}} \quad (6)$$

In the presence of alkali metal ions, the L^- and ML species are taken into consideration at the heptane/water interface. Thus, eq 6 is rewritten as follows:

$$D = \frac{\chi_{zzz}}{\chi_{zzz} + 2\chi_{xxz}} = \frac{N_{s,L^-}\beta_{zzz,L^-}\langle\cos^3\theta_{L^-}\rangle + N_{s,ML}\beta_{zzz,ML}\langle\cos^3\theta_{ML}\rangle}{N_{s,L^-}\beta_{zzz,L^-}\langle\cos\theta_{L^-}\rangle + N_{s,ML}\beta_{zzz,ML}\langle\cos\theta_{ML}\rangle}$$

$$= \frac{(1-\alpha)\langle\cos^2\theta_{L^-}\rangle + \alpha\langle\cos^3\theta_{ML}\rangle}{(1-\alpha)\langle\cos\theta_{L^-}\rangle + \alpha\langle\cos\theta_{ML}\rangle} \quad (7)$$

$$\alpha = \frac{N_{s,ML}}{N_{s,L} + N_{s,ML}} \quad (8)$$

where θ_{L^-} and θ_{ML} are the orientation angles of L^- and ML, and α represents the mole fraction of ML at the heptane/water interface. Since there is no UV−Vis spectral change of azoprobe **1** in the presence of alkali metal ions (Figure 2), it can be assumed that $\beta_{zzz,L^-} = \beta_{zzz,ML}$.

Because the Fresnel coefficients also depend on the relative optical dielectric constants of the monolayer at the wavelengths of the fundamental (ϵ_m(532 nm)) and second-harmonic beams (ϵ_m(266 nm)), these dielectric constants must be determined by another method. When the dominant molecular hyperpolarizability tensor element for azoprobe **1** is mainly based on β_{zzz}, the ratio of ϵ_m(532 nm) to ϵ_m(266 nm) is calculated from the SH intensity ratio for the *s*-polarized fundamental input/*p*-polarized SHG output to the 45°-polarized fundamental input/*s*-polarized SHG output.[39] Since the molar absorptivity of azoprobe **1** at the SH wavelength is small, the ϵ_m(266 nm) value is estimated to be the average of the relative optical dielectric constants between two bulk phases as recently reported.[3,4] Based on this assumption, the orientation parameter values (*D*) calculated from eq 7 are summarized in Table 2. For the TMA^+ system, the orientation angle of L^- is calculated as 31° against the surface normal from eq 6. Although the solvent systems are different, the observed θ value agrees well with that of 4-(4′-

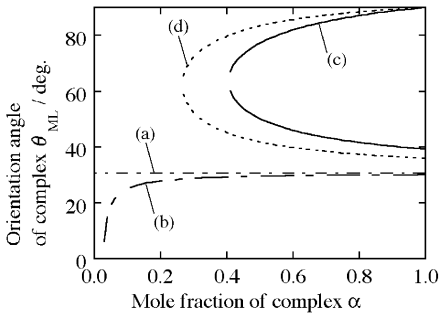

Figure 5. Orientation angle of complexes θ_{ML} as a function of the mole fraction of complex α, simulated by using the orientation parameter D (θ_{L^-} is constant): (a) TMACl, (b) LiCl, (c) NaCl, (d) KCl.

TABLE 2: Orientation Parameter *D* and Orientation Angle *θ*

	D	*θ*/degree
TMACl	0.74	31
LiCl	0.75	
NaCl	0.60	
KCl	0.66	

dodecyloxyazobenzene)benzoic acid ($\theta = 29°$) and *p*-dimethylamino-azobenzene sulfonate ($\theta = 34°$) at the 1,2-dichloroethane/water.[28,30] In the presence of alkali metal ions, the θ values of L^- and ML cannot be calculated because three uncertain constants (α, θ_{L^-}, and θ_{ML}) remain.

Since no SHG spectral shifts in Figure 2A is noted upon addition of alkali metal salts for azoprobe **1**, the interaction between azoprobes at the interface must be small. Thus the orientation angle of L^- (θ_{L^-}) is estimated to be constant even in the presence of ML species, and the relationship between θ_{ML} and α under constant θ_{L^-} can be simulated using D values listed in Table 2. The simulation results are shown in Figure 5. It is evident that the orientation angle of ML (θ_{ML}) is larger for Na^+ and K^+ as compared with θ_{L^-}, whereas the θ_{ML} for Li^+ is smaller in every α fractions. This result clearly demonstrates that the Na^+ and K^+ complexes are flatter and the Li^+ complex tends to lift up at the heptane/water interface as compared with the orientation angle of L^- species. The observed orientation changes of ML species may be ascribed to the difference in the charge distribution of alkali metal ion complexes formed at the interface. Since Na^+ and K^+ can form tight ion pairs with azoprobe **1** based on the best size-fitting with the 15-crown-5 binding site,[38] charge delocalized complexes, which induce the flatter orientation at the interface, are expected. On the other hand, Li^+ ion is too small to fit inside the 15-crown-5 cavity. Thus the highly hydrated Li^+ complex makes the binding site of azoprobe **1** more hydrophilic, resulting in the lift-up conformation at the heptane/water interface. Figure 5 also indicates that there are two possible values for the orientation angle θ_{ML} for Na^+ and K^+ complexes; θ_{ML} values of ca. 40° and ca. 80° above $\alpha = 0.5$. Although both angles are theoretically feasible, the angle change from 31° for L^- to ca. 80° for ML complexes at the interface seems to be too drastic.

The simulation in Figure 5 also suggests that the mole fractions α should be greater than 0.41 for the Na^+ complex and 0.27 for the K^+ complex. This is supported by the fact that the SH intensities upon addition of NaCl and KCl are 2.5−3 times larger than that for TMACl, indicating the larger distribution of Na^+ and K^+ complexes at the heptane/water interface compared with the free L^- species. As for the Li^+ complex, the mole fraction of Li^+ complex at the heptane/water interface must be low, since the increase of SH intensity for the Li^+ complex is small (Figure 2). As shown in Figure 5(b), when the α value for the Li^+ complex is less than 0.1, the θ_{ML} value decreases steeply and the small θ_{ML} value means lift-up orientation of ML species at the heptane/water interface. These orientation differences among the alkali metal complexes offer a unique characteristic for molecular recognition at the liquid/liquid interface, which is clarified for the first time by the present SHG spectroscopy study.

Conclusion

This study demonstrated alkali metal ion recognition with crown ether azoprobe **1** at the heptane/water interface using SHG spectroscopy analysis. It was found that an increase of the SH intensity reflected the extractability of alkali metal complexes with azoprobe **1** from the aqueous phase into the heptane/water interface. The red shift of SHG spectra for azoprobe **1** revealed that the heptane/water interface provided an intermediate polarity between the two solvents. In such a specific medium, even the hydrated Li^+ complexes could be distributed; this fact was elucidated by the increase of the SH intensity for LiCl in comparison with the TMACl system at the heptane/water interface. The light polarization analysis of the SH intensity exhibited a clear change in the orientation angle of alkali metal complexes at the heptane/water interface. It was found that the Na^+ and K^+ complexes were flatter while the Li^+ complex had the lift-up orientation at the heptane/water interface as compared with the orientation angle of the L^- species. Thus, the dynamic orientation change of azoprobe **1** in alkali metal ion recognition at the heptane/water interface has been clarified for the first time by SHG spectroscopy. It is expected that the present results will provide useful information for novel molecular recognition processes at the liquid/liquid interfaces in combination with computer simulations at liquid interfaces. Some of these approaches are being actively followed in the authors' laboratory.

Acknowledgment. The authors thank Profs. M. Takagi and Y. Katayama (Kyushu University) for providing the azoprobe **1**. This research was supported by a Grant-in-Aid for Scientific Research (Nos. 13129201, 14204074, and 14340230) from the Ministry of Education, Science, Sports, and Culture, Japan.

References and Notes

(1) Bessho, K.; Uchida, T.; Yamauchi, A.; Shioya, T.; Teramae, N. *Chem. Phys. Lett.* **1997**, *264*, 381.
(2) Wang, H.; Borguet, E.; Eisenthal, K. B. *J. Phys. Chem. A* **1997**, *101*, 713.
(3) Wang, H.; Borguet, E.; Eisenthal, K. B. *J. Phys. Chem. B* **1998**, *102*, 4927.
(4) Ishizaka, S.; Kim, H.-B.; Kitamura, N. *Anal. Chem.* **2001**, *73*, 2421.
(5) Du, Q.; Freysz, E.; Shen, Y. R. *Science* **1994**, *264*, 826.
(6) Miranda, P. B.; Shen, Y. R. *J. Phys. Chem. B* **1999**, *103*, 3292.
(7) Ishizaka, S.; Habuchi, S.; Kim, H.-B.; Kitamura, N. *Anal. Chem.* **1999**, *71*, 3382.
(8) Uchida, T.; Yamaguchi, A.; Ina, T.; Teramae, N. *J. Phys. Chem. B* **2000**, *104*, 12091.
(9) Ariga, K.; Kunitake, T. *Acc. Chem. Res.* **1998**, *31*, 371.
(10) Nishizawa, S.; Yokobori, T.; Shioya, T.; Teramae, N. *Chem. Lett.* **2001**, 1058.
(11) Nishizawa, S.; Yokobori, T.; Kato, R.; Shioya, T.; Teramae, N. *Bull. Chem. Soc. Jpn.* **2001**, *74*, 2343.
(12) Shigemori, K.; Nishizawa, S.; Yokobori, T.; Shioya, T.; Teramae, N. *New J. Chem.* **2002**, *26*, 1102.
(13) Shioya, T.; Nishizawa, S.; Teramae, N. *J. Am. Chem. Soc.* **1998**, *120*, 11534.
(14) Kral, V.; Sessler, J. L.; Shishkanova, T. V.; Gale, P. A.; Volf, R. *J. Am. Chem. Soc.* **1999**, *121*, 8771.
(15) Umezawa, Y. In *Liquid Interfaces in Chemical, Biological, and Pharmaceutical Applications*; Volkov, A. G., Ed.; Marcel Dekker: New York, 2001; Vol. 95, p 439.

(16) Girault, H. H. In *Modern Aspects of Electrochemisty*; White, R. E., Conway, B. E., Bockris, J. O., Eds.; Plenum: New York, 1993; Vol. 25, p 31.
(17) Kakiuchi, T. In *Liquid Interfaces in Chemical, Biological, and Pharmaceutical Applications*; Volkov, A. G., Ed.; Marcel Dekker: New York, 2001; Vol. 95, p 105.
(18) Volkov, A. G. *Anal. Sci.* **1998**, *14*, 19.
(19) Liu, B.; Mirkin, M. V. *Electroanalysis* **2000**, *12*, 1433.
(20) Crawford, M. J.; Frey, J. G.; VanderNoot, T. J.; Zhao, Y. *J. Chem. Soc., Faraday Trans.* **1996**, *92*, 1369.
(21) Kakiuchi, T.; Ono, K.; Takasu, Y.; Bourson, J.; Valeur, B. *Anal. Chem.* **1998**, *70*, 4152.
(22) Shen, Y. R. *The Principles of Nonlinear Optics*; John Wiley & Sons: New York, 1984.
(23) Heinz, T. F. In *Modern Problems in Condensed Matter Sciences*; Ponath, H.-E., Stegman, G. I., Eds.; Elsevier: Amsterdam, 1991; Vol. 29, p 353.
(24) Eisenthal, K. B. *Chem. Rev.* **1996**, *96*, 1343.
(25) Corn, R. M.; Higgins, D. A. *Chem. Rev.* **1994**, *94*, 107.
(26) Brevet, P. F.; Girault, H. H. In *Liquid−Liquid Interfaces Theory and Methods*; Volkov, A. G., Deamer, D. W., Eds.; CRC Press: New York, 1996; p 103.
(27) Heinz, T. F.; Chen, C. K.; Ricard, D.; Shen, Y. R. *Phys. Rev. Lett.* **1982**, *48*, 478.
(28) Rinuy, J.; Piron, A.; Brevet, P. F.; Blanchard-Desce, M.; Girault, H. H. *Chem. Eur. J.* **2000**, *6*, 3434.
(29) Yamaguchi, A.; Uchida, T.; Teramae, N.; Kaneta, H. *Anal. Sci.* **1997**, *13*, 3, suppl., 85.
(30) Naujok, R. R.; Higgins, D. A.; Hanken, D. G.; Corn, R. M. *J. Chem. Soc., Faraday Trans.* **1995**, *91*, 1411.
(31) Conboy, J. C.; Daschbach, J. L.; Richmond, G. L. *J. Phys. Chem.* **1994**, *98*, 9688.
(32) Katayama, Y.; Nita, K.; Ueda, M.; Nakamura, H.; Takagi, M. *Anal. Chim. Acta* **1984**, *173*, 193.
(33) Izatt, R. M.; Bradshow, J. S.; Nielsen, S. A.; Lamb, J. D.; Christensen, J. J.; Sen, D. *Chem. Rev.* **1985**, *85*, 271.
(34) Yam, R.; Berkovic, G. *Langmuir* **1993**, *9*, 2109.
(35) Kimura, K.; Tanaka, M.; Iketani, S.; Shono, T. *J. Org. Chem.* **1987**, *52*, 836.
(36) Kasha, M.; Rawls, H. R.; El-Bayoumi, M. A. *Pure Appl. Chem.* **1965**, *11*, 371.
(37) Tamburello-Luca, A. A.; Herbert, P.; Antoine, R.; Brevet, P. F.; Girault, H. H. *Langmuir* **1997**, *13*, 4428.
(38) Hayashita, T.; Takagi, M. In *Comprehensive Supramolecular Chemistry*; Gokel, G. W., Ed.; Pergamon: New York, 1996; Vol. 1, p 635.
(39) Zhang, T. G.; Zhang, C. H.; Wong, G. K. *J. Opt. Soc. Am. B* **1990**, *7*, 902.